Unraveling the Complexities of Hepatitis B Virus Control: A Mathematical Modeling Approach

Wiley
Journal of Mathematics
Volume 2025, Article ID 6616833, 13 pages
https://doi.org/10.1155/jom/6616833

WILEY

Research Article

Unraveling the Complexities of Hepatitis B Virus Control: A Mathematical Modeling Approach

Malik Muhammad Ibrahim,[1] **Jong Hyuk Byun**,[2,3] **Malik Muhammad Naeem Mannan**,[4,5] **Il Hyo Jung**,[2,3] **and Kwang Su Kim**[1]

[1]*Department of Scientific Computing, Pukyong National University, Busan, Republic of Korea*
[2]*Department of Mathematics and Institute of Mathematical Sciences, Pusan National University, Busan, Republic of Korea*
[3]*Institute for Future Earth, Pusan National University, Busan 46241, Republic of Korea*
[4]*Griffith Center of Biomedical and Rehabilitation Engineering (GCORE), Griffith University, Gold Coast, Australia*
[5]*School of Health Sciences and Social Work, Griffith University, Gold Coast, Australia*

Correspondence should be addressed to Kwang Su Kim; kwangsukim@pknu.ac.kr

Received 22 July 2024; Revised 28 August 2025; Accepted 4 September 2025

Academic Editor: Pramita Mishra

Hepatitis B virus (HBV) infection remains a major health challenge due to the persistence of covalently closed circular DNA (cccDNA), which acts as a reservoir for viral replication and hinders complete cure. Existing mathematical models have offered valuable insights into HBV dynamics, but the independent role of cccDNA recycling has not been clearly isolated, as most studies embed these processes within complex immune responses or therapy-focused frameworks. To address this gap, we developed a mathematical model that distinguishes between hepatocytes carrying single and multiple copies of cccDNA, thereby capturing intracellular heterogeneity that is often overlooked. Using a system of four differential equations, we derived the basic reproduction number (R_0) through the next-generation matrix method and analyzed the stability of both disease-free and endemic equilibria. Numerical simulations, including bifurcation and sensitivity analyses, were conducted to evaluate the impact of key parameters on HBV persistence. The results demonstrate that the recycling parameter associated with single-copy cccDNA plays a dominant role in reducing HBV persistence compared to transitions involving multiple-copy states. These findings underscore the importance of accounting for cccDNA burden at the cellular level and provide theoretical insights that may guide the design of antiviral strategies targeting early infection stages.

Keywords: basic reproductive number; covalently closed circular DNA (cccDNA); hepatitis B virus (HBV)

1. Introduction

Hepatitis B virus (HBV) is a DNA virus belonging to the Hepadnaviridae family that exclusively infects humans. Transmission occurs mainly through exposure to infected blood and sexual contact, and infection can result in a spectrum of clinical outcomes, ranging from asymptomatic carriage to acute self-limiting hepatitis, fulminant hepatitis, and chronic disease [1, 2]. Worldwide, more than two billion people have been exposed to HBV, with approximately 240 million living with chronic infection, making it a major contributor to illness and mortality in high-prevalence regions [3]. People with acute hepatitis B may experience symptoms such as jaundice, fever, abdominal discomfort, nausea, vomiting, and hepatosplenomegaly [1, 4, 5].

In the HBV replication process, the virus gains entry into liver cells by attaching to the NTCP receptor on their surface [6–8]. Once inside, the viral DNA is transported to the nucleus, where it is converted into covalently closed circular DNA (cccDNA), which functions as the template for viral

RNA synthesis [9]. These RNAs are used to produce new viral particles that are either secreted or recycled within the cell to sustain infection [10, 11].

In most cases, acute HBV infection resolves spontaneously; therefore, antiviral treatment is typically recommended for individuals with chronic infection [12]. A central step in HBV replication is the production of new viral DNA genomes through the reverse transcription of RNA pregenomes derived from cccDNA in the cytoplasm [13–16]. cccDNA is also replenished during intracellular recycling and plays a crucial role in the early stages of infection [17, 18].

cccDNA is the principal reservoir enabling persistent HBV infection, residing in the nuclear compartment of infected hepatocytes and serving as a template for viral transcription and replication [19–21]. The persistence of HBV is largely due to the stable and tightly regulated presence of this episomal form of the viral genome within infected cell nuclei [22]. Recent studies indicate that the inability of current therapeutic approaches to completely eliminate nuclear cccDNA is a major barrier to achieving a functional cure [23–26]. After HBV enters the host, its DNA is initially converted into a single cccDNA molecule, which can then amplify to as many as 50 copies [16]. Elucidating the turnover rate of existing cccDNA pools is essential for designing strategies aimed at eradicating HBV by preventing the generation of new cccDNA molecules [19].

Mathematical modeling is an essential tool for analyzing the transmission and control of infectious diseases, and recent studies have applied advanced numerical methods and stability analyses to HBV dynamics [27, 28]. A pioneering contribution by Nowak et al. introduced a basic model to assess the effectiveness of antiviral therapy in reducing viral load [29]. Since then, a variety of modeling strategies such as stochastic control methods, bifurcation analysis of stochastic epidemic models, fractional-order systems with complex boundary conditions, and noise-driven epidemic dynamics have been employed to capture diverse aspects of disease spread [30–35]. Recent developments have extended these frameworks to nonlinear, fractional-order, and drug-responsive systems in biomedical applications [36–39]. In the context of HBV, some models have examined the interaction between antiviral therapy and infection dynamics, incorporating factors such as drug efficacy and pharmacokinetics (PKs) [29, 40–42], while other models investigated the effects of time lag or spatial spread, considering the time from infection to the spread of free viral particles and their migration within the liver [43–46]. These approaches provide powerful methodological foundations for developing biologically realistic HBV models.

Several studies have explored the interactions between different populations of infected hepatocytes harboring varying numbers of cccDNA copies [47, 48]. Li et al. proposed a mathematical model to evaluate the interplay between cccDNA and dendritic cells in chronic HBV infection, concluding that long-term continuous therapy is critical for symptom reduction and sustained treatment effectiveness [47]. In another work, Ciupe et al. developed a model that categorized infected hepatocytes into two groups: those containing a single cccDNA copy and those with multiple copies [48].

In this study, we present a novel mathematical model of HBV infection that captures key intracellular processes by partitioning hepatocytes into distinct compartments according to their cccDNA load, without explicitly incorporating $CD8^+$ T-cell dynamics. The model distinguishes between uninfected hepatocytes (T), singly infected hepatocytes carrying one copy of cccDNA (I_1), multiply infected hepatocytes with multiple cccDNA copies (I_2), and free virus (V). This distinction reflects biological evidence showing that the number of cccDNA copies per cell influences the persistence and reactivation potential of HBV. In our model, parameter ρ_1 represents the rate at which multiply infected cells (I_2) revert to singly infected cells (I_1), which may occur due to partial immune-mediated clearance or degradation of excess cccDNA copies. Conversely, ρ_2 denotes the rate at which singly infected cells acquire additional cccDNA copies and transition into the I_2 class, representing the effect of secondary infection events or cccDNA amplification within the host cell. These recycling transitions model intracellular dynamics that are often overlooked in conventional HBV models but are crucial for understanding viral persistence and the difficulty of achieving a complete cure.

To assess the potential for infection spread, we derive the basic reproduction number R_0 using the next-generation matrix method. This threshold parameter governs the global dynamics of the system: if $R_0 < 1$, the disease-free equilibrium (DFE) is locally asymptotically stable, indicating that infection cannot persist in the population. In contrast, when $R_0 > 1$, the system admits a stable endemic equilibrium (EE), representing a chronic infection state. These theoretical findings are supported by numerical simulations. We also conduct a bifurcation analysis with respect to the transmission rate β to investigate how variations in infection strength influence the system's behavior. The results show that small changes in β can lead to significant shifts in long-term outcomes. Furthermore, sensitivity analysis is performed to determine which parameters most strongly affect R_0, providing insight into the mechanisms that drive infection persistence. Notably, parameters ρ_1 and β emerge as influential, suggesting that therapeutic strategies aimed at enhancing cccDNA clearance or limiting reinfection may offer effective control of HBV. This model thus provides a refined framework for investigating HBV dynamics and contributes to the development of targeted antiviral interventions.

2. Mathematical Model of HBV Dynamics With cccDNA Heterogeneity

Based on the infection and intracellular dynamics illustrated in Figure 1, the proposed model can be formulated using the following system of ordinary differential equations [48, 49]:

$$\frac{dT}{dt} = S - d_T - \beta TV + \rho_1 I_1, \tag{1}$$

$$\frac{dI_1}{dt} = \beta TV - \rho_1 I_1 + \rho_2 I_2 - zI_1 - d_I I_1, \tag{2}$$

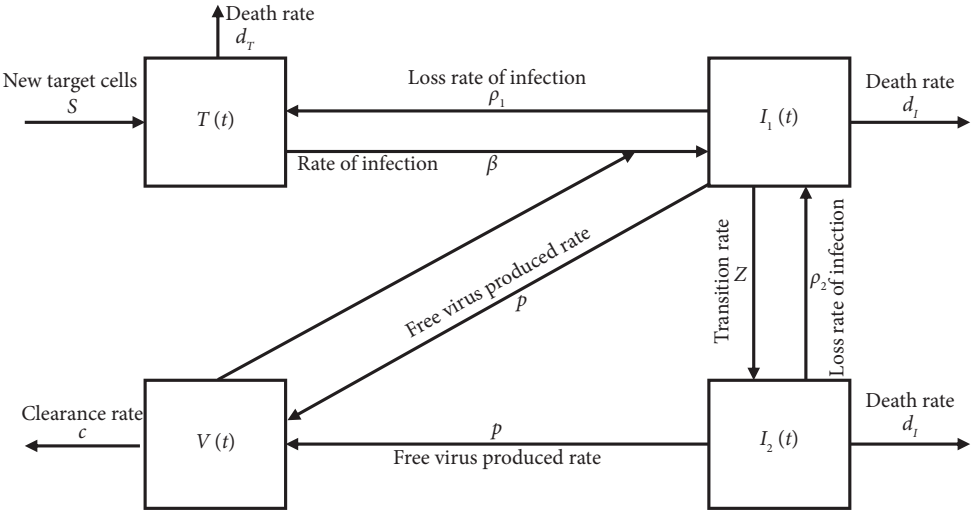

FIGURE 1: Schematic diagram of the proposed HBV infection model incorporating intracellular recycling dynamics. The model categorizes hepatocytes into four compartments: uninfected cells (T), infected cells with a single copy of cccDNA (I_1), infected cells with multiple copies of cccDNA (I_2), and free virus (V). Uninfected cells (T) become infected at a rate β through interaction with virus particles, and infected cells can transition between I_1 and I_2 through intracellular mechanisms. The parameter ρ_2 represents the rate of cccDNA accumulation ($I_1 \longrightarrow I_2$), while ρ_1 denotes partial clearance or reduction in cccDNA copies ($I_2 \longrightarrow I_1$). Both infected cells die at rate d_I, while producing virus particles at rates p. Both I_1 and I_2 produce new virus particles, which are cleared at rate c. This model structure captures both infection dynamics and intracellular complexity of cccDNA burden, which are critical for understanding HBV persistence and treatment dynamics.

$$\frac{dI_2}{dt} = zI_1 - \rho_2 I_2 - d_I I_2, \tag{3}$$

$$\frac{dV}{dt} = pI_1 + pI_2 - cV. \tag{4}$$

We proposed a mathematical model that describes the within-host dynamics of HBV infection, focusing on the interaction between uninfected hepatocytes, infected cells carrying different levels of cccDNA, and free virus. The model includes four compartments: uninfected hepatocytes (T), infected hepatocytes with a single copy of cccDNA (I_1), infected hepatocytes with multiple copies of cccDNA (I_2), and free virus (V).

Uninfected hepatocytes (T) are produced at a constant source rate S, die at rate d_T, and become infected by interacting with free virus (V) at a rate proportional to βTV, where β is the infection rate and the interaction term βTV describes the infection process, where uninfected hepatocytes (T) come into contact with free virus (V), leading to the production of infected cells with a single copy of cccDNA (I_1). These cells may either be cleared noncytolytically and revert to the uninfected class at rate ρ_1, or acquire additional cccDNA and transition to the I_2 class at rate z or be cleared at rate d_I. The I_2 class includes cells with multiple cccDNA copies, which may revert to the I_1 class at rate ρ_2 or be cleared at rate d_I. The virus is produced from both infected cell compartments at rate p and cleared from the system at rate c. This structure captures the intracellular heterogeneity of HBV infection, particularly the distinction between single- and multiple-copy cccDNA burdens. It is important to note that ρ_1 and ρ_2 represent intracellular transition rates between infected cell states (I_1 and I_2) and do not involve the free virus compartment (V). Therefore, they do not appear in the differential equation for V. Although ρ_1 and ρ_2 describe biological changes in infected cells, they should not be confused with the infection rate β, which governs viral transmission between free virus and uninfected cells. The full system of differential equations governing these interactions is provided below, and the biological meanings of all parameters are summarized in Table 1.

3. Identification of DFE and Endemic Equilibria

DFEs are stable conditions under which no cells are infected. To analyze the steady-state behavior of the system, we determine the equilibrium points by setting the right-hand sides of all differential equations equal to zero. That is, we solve $(dT/dt) = 0$, $(dI_1/(dt)) = 0$, $(dI_2/(dt)) = 0$, and $(dV/dt) = 0$. Solving the equations leads to DFE points, which are denoted as E_0, $E_0 = (T_0, I_{1_0}, I_{2_0}, V_0) = (S/d_T, 0, 0, 0)$. Mathematically, an infected steady state or EE always exists; however, the biological significance of this state depends on R_0. If $R_0 > 1$, the system reaches EE. EE is found by solving the system at steady state, assuming all state variables are positive. Solving the equations leads to the EE point $E^* = (T^*, I_1^*, I_2^*, V^*)$, where $T^* = (c((d_I + \rho_1)(d_I + \rho_2) + zd_I))/(\beta p(\rho_2 + z + d_I))$, $I_1^* = (S(d_I+\rho_2)(1 - 1/R_0))/(d_I(d_I + \rho_2 + z))$, $I_2^* = (Sz(1 - 1/R_0))/(d_I(d_I+\rho_2 + z))$, and $V^* = Sp(1 - 1/R_0)/cd_I$.

4. Derivation of Basic Reproduction Number R_0 and Its Epidemiological Interpretation

In this section, we derive the basic reproduction number R_0, which serves as a threshold parameter governing the long-term behavior of the HBV infection. Mathematically, R_0 is defined as the expected number of new infected hepatocytes

Table 1: Model parameters and initial values used in the HBV infection dynamics simulation.

Parameter or variable	Symbol	Unit	Values	Reference
Produced new uninfected hepatocyte cells	S	Cell/mL/day	5×10^{5}	[49]
Death rate of uninfected hepatocytes	d_T	Day^{-1}	0.0003	[49]
Rate of infection	β	mL/virions/day	0.9×10^{-10}	[48]
Recycling rate of hepatocytes infected with a single cccDNA copy (I_1) back toward the uninfected hepatocyte	ρ_1	Virions/cell/day	0.12	[48]
Recycling rate of hepatocytes infected with multiple cccDNA copies (I_2) reverting to the single-copy infected state (I_1)	ρ_2	Virions/cell/day	0.05	[48]
Transition rate into the I_2 class	z	Day^{-1}	0.84	
Death rate of infected hepatocytes	d_I	Day^{-1}	0.043	[49]
Free virus produced rates	p	Virions/mL/day	6.24	[49]
Virus clearance rate	c	Day^{-1}	0.67	[48]
Uninfected hepatocytes	$T(0)$	Cells/mL	13.6×10^{6}	[48]
Infected hepatocytes (I_1)	$I1(0)$	Cells/mL	0	[48]
Infected hepatocytes (I_2)	$I2(0)$	Cells/mL	0	[48]
Free virus	$V(0)$	Particles/mL	0.33	[48]

generated by a single infected cell in a completely susceptible environment. We employ the next-generation matrix method to compute R_0, focusing on the compartments associated with intracellular viral activity specifically, hepatocytes carrying single and multiple copies of cccDNA. Biologically, if $R_0 < 1$, the infection will eventually be cleared, and the DFE is locally asymptotically stable. Conversely, if $R_0 > 1$, the infection can persist, leading to the establishment of an EE. This threshold captures how cccDNA amplification and intercellular viral spread collectively drive infection dynamics, and it provides a basis for evaluating intervention strategies aimed at reducing viral persistence.

To compute R_0 for the system of equations (1)–(4), we used the next-generation matrix technique described in [50]. Where $x = \begin{pmatrix} I_1 & I_2 & V \end{pmatrix}^T$, then the model equations can be written as $(dx/dt) = F(x) - V(x)$, where $V(x) = (V^-(x) - V^+(x))$:

$$F(x) = \begin{pmatrix} \beta TV \\ 0 \\ 0 \end{pmatrix}, \qquad V(x) = \begin{pmatrix} \rho_1 I_1 + zI_1 + d_I I_1 - \rho_2 I_2 \\ \rho_2 I_2 + d_I I_2 - zI_1 \\ cV - pI_1 - pI_2 \end{pmatrix}. \tag{5}$$

Taking the partial derivative of F and V at DFE points,

$$F = \begin{pmatrix} 0 & 0 & \beta\dfrac{S}{d_T} \\ 0 & 0 & 0 \\ 0 & 00 & 0 \end{pmatrix}, \qquad V = \begin{pmatrix} \rho_1 + z + d_I & -\rho_2 & 0 \\ -z & \rho_2 + d_I & 0 \\ -p & -p & c \end{pmatrix}, \tag{6}$$

so that

$$V^{-1} = \frac{1}{\left((\rho_1 + d_I)(\rho_2 + d_I) + d_I z\right)} \begin{bmatrix} (\rho_2 + d_I) & (\rho_2 - p) & 0 \\ z & (\rho_1 + z + d_I) & 0 \\ \dfrac{z(p + \rho_2 + d_I)}{c} & \dfrac{p(\rho_1 + z + d_I + \rho_2)}{c} & \dfrac{\left((\rho_1 + d_I)(\rho_2 + d_I) + d_I z\right)}{c} \end{bmatrix}. \tag{7}$$

The basic reproductive number $R_0 = \rho(FV^{-1})$ is the spectral radius of the product FV^{-1}, and thus, $R_0 = (\beta Sp(\rho_2 + z + d_I))/(cd_T((d_I + \rho_1)(d_I + \rho_2) + zd_I))$.

5. Local Stability of the DFE and Endemic Equilibria Based on R_0

In this section, we investigate the local stability of the two equilibrium points of the proposed HBV model: the DFE and the EE. To determine the stability conditions, we first compute the Jacobian matrix of the system and evaluate it at each equilibrium. The resulting characteristic equations are analyzed using the Routh–Hurwitz stability criteria, which provide necessary and sufficient conditions for all eigenvalues to have negative real part ensuring local asymptotic stability. Based on this approach, we formulate and prove two theorems: The DFE is locally asymptotically stable when the basic reproduction number satisfies $R_0 < 1$, and the EE becomes locally stable when $R_0 > 1$, assuming all Routh–Hurwitz conditions are met. These results reinforce the interpretation of R_0 as a critical threshold that governs whether the infection will die out or persist over time.

Theorem 1. *The DFE E_0 is locally asymptotically stable when $R_0 < 1$, and $\beta Sp < d_T((d_I + \rho_1)(d_I + \rho_2) + d_I z)$ and E_0 is unstable when $R_0 > 1$.*

Proof 1. The Jacobian matrix of E_0 is given by

$$J(E_0) = \begin{bmatrix} -d_T & \rho_1 & 0 & -\frac{\beta S}{d_I} \\ 0 & -\rho_1 - z - d_I & \rho_2 & \frac{\beta S}{d_I} \\ 0 & z & -\rho_2 - d_I & 0 \\ 0 & p & p & -c \end{bmatrix}. \quad (8)$$

□

The eigenvalues of $J(E_0)$ are the solutions of the characteristic equation of

$$P(\lambda) = \lambda^4 + a_1\lambda^3 + a_2\lambda^2 + a_3\lambda + a_4, \quad (9)$$

with constants

$$\begin{aligned} a_1 &= (c + 2d_I + d_T + \rho_1 + \rho_2 + z), \\ a_3 &= c((d_I + \rho_1)(d_I + \rho_2) + zd_I)(1 - R_0) + \{d_T((d_I + \rho_1)(d_I + \rho_2) + d_I z) - \beta Sp\} + cd_T(z + 2d_I + \rho_2 + d_I + \rho_1), \\ a_4 &= d_T c((d_I + \rho_1)(d_I + \rho_2) + zd_I)(1 - R_0). \end{aligned} \quad (10)$$

When $R_0 < 1$ and $\beta Sp < d_T((d_I + \rho_1)(d_I + \rho_2) + d_I z)$, the conditions $a_1 > 0$, $a_3 > 0$, and $a_4 > 0$ are satisfied. Under the Routh–Hurwitz stability criterion, for all roots of the polynomial to have negative real parts, it is required that $a_i > 0$, for $i = 1, 2, 3, 4$, and that the inequality $a_5 = a_1 a_2 a_3 - a_3^2 - a_1^2 a_4 > 0$ must also be satisfied. Let $a_5 = AB > 0$, where

$$\begin{aligned} A &= a_3 + d_T^2(c + 2d_I + \rho_1 + \rho_2 + z + d_T), \\ B &= \frac{(c + d_I + \rho_1)}{d_T}\{d_T((d_I + \rho_1)(d_I + \rho_2) + zd_I) - \beta ps\} + ((d_I + \rho_1)(d_I + \rho_2) + zd_I)(c + \rho_2 + z) \\ &\quad + (2d_I + \rho_1 + \rho_2 + z)(cd_I + c^2) + (d_I + 2z)(c\rho_1 + c\rho_2) + c(\rho_1^2 + \rho_2^2 + z^2). \end{aligned} \quad (11)$$

When $R_0 < 1$ and $\beta Sp < d_T((d_I + \rho_1)(d_I + \rho_2) + d_I z)$, $a_5 > 0$.

The characteristic polynomial of the Jacobian matrix is evaluated at the DFE. The coefficients a_1, a_3, a_4, and a_5 are positive and satisfying the stability requirement. This confirms that the DFE E_0 is locally asymptotically stable if $R_0 < 1$ and $\beta Sp < d_T((d_I + \rho_1)(d_I + \rho_2) + d_I z)$. However, when $R_0 > 1$, the coefficient a_4 becomes negative, violating the Routh–Hurwitz conditions. As a result, E_0 becomes unstable when $R_0 > 1$.

Theorem 2. *The EE E^* is locally asymptotically stable if $R_0 > 1$ and $(JUL)/cd_I(d_I + \rho_2 + z) > (QJ^2 + U^2)$. E^* is unstable when $R_0 < 1$.*

Proof 2. The Jacobian matrix of E^* is given by

$$J(E^*) = \begin{bmatrix} -d_T - \dfrac{\beta Sp(1-1/R_0)}{cd_I} & \rho_1 & 0 & -\dfrac{c((d_I+\rho_1)(d_I+\rho_2)+zd_I)}{p(d_I+\rho_2+z)} \\ \dfrac{\beta Sp(1-1/R_0)}{cd_I} & -\rho_1 - z - d_I & \rho_2 & \dfrac{c((d_I+\rho_1)(d_I+\rho_2)+zd_I)}{p(d_I+\rho_2+z)} \\ 0 & z & -\rho_2 - d_I & 0 \\ 0 & p & p & -c \end{bmatrix}. \tag{12}$$

□

The eigenvalues of $J(E_0)$ are the solution of the characteristic equation

$$P(\lambda) = \lambda^4 + k_1\lambda^3 + k_2\lambda^2 + k_3\lambda + k_4, \tag{13}$$

with constants $k_1 = (A+B)/(cd_I(d_I+\rho_2+z))$, $k_3 = (C+D+E+F+G)/(cd_I(d_I+\rho_2+z))$, and $k_4 = H$, where

$$\begin{aligned} A &= cd_I\{c(d_I+\rho_2+z) + d_I(2d_I+3\rho_2+3z+\rho_1) + \rho_2(\rho_2+\rho_1) + z(2\rho_2+z+\rho_1)\}, \\ B &= ps\beta(d_I+\rho_2+z) - cd_T(d_I\rho_1+\rho_1\rho_2), \\ C &= cd_I\{cd_T((d_I+\rho_1)(d_I+\rho_2)+zd_I)(R_0-1)\}, \\ D &= cd_I\{ps\beta(d_I+\rho_2+z) - cd_T(d_I\rho_1+\rho_1\rho_2)\}, \\ E &= c\rho_2\{ps\beta(d_I+\rho_2+z) - cd_T(d_I\rho_1+\rho_1\rho_2)\}, \\ F &= cz\{ps\beta(d_I+\rho_2+z) - cd_T\rho_1\rho_2\}, \\ G &= ps\beta d_I\{d_I^2 + \rho_2(2d_I+\rho_2) + z(2d_I+2\rho_2+z)\}, \\ H &= cd_T((d_I+\rho_1)(d_I+\rho_2)+zd_I)(R_0-1). \end{aligned} \tag{14}$$

When $R_0 > 1 \Longrightarrow \beta Sp(\rho_2+z+d_I) > cd_T((d_I+\rho_1)(d_I+\rho_2)+zd_I) > cd_T(d_I\rho_1+\rho_1\rho_2) > cd_T\rho_1\rho_2$. So, $A>0$, $B>0$, $C>0$, $D>0$, $E>0$, $F>0$, $G>0$, and $H>0$, when $R_0>1$. This implies that when $R_0>1$, $k_1>0$, $k_3>0$, and $k_4>0$. According to the Routh–Hurwitz stability criterion, a necessary condition for all the roots of the polynomial to have negative real part is that all coefficient $k_i > 0$, for $i = 1, 2, 3, 4$, and that the following inequality also holds $k_5 = k_1k_2k_3 - k_3^2 - k_1^2k_4 > 0$:

$$K_5 = \frac{1}{c^2d_I^2(d_I+\rho_2+z)^2}\left\{\frac{JUL}{cd_I(d_I+\rho_2+z)} - (QJ^2+U^2)\right\}, \tag{15}$$

where $J = A+B$, $Q = H$,

$$\begin{aligned} U &= \{c^2d_Id_T((d_I+\rho_1)(d_I+\rho_2)+zd_I)(R_0-1) + (ps\beta(d_I+\rho_2+z)) - cd_T(d_I\rho_1+\rho_1\rho_2)(cd_I+c\rho_2) \\ &\quad + cz(ps\beta(d_I+\rho_2+z) - cd_T\rho_1\rho_2) + ps\beta d_I(d_I(d_I+2\rho_2+2z)) + \rho_2^2 + z(2\rho_2+z)\}, \\ L &= [cd_I\{c(d_I(d_I+2\rho_2+2z) + z(2\rho_2+z+\rho_1) + \rho_2^2) + d_I(\rho_2(\rho_2+2z+2\rho_1) + z(z+\rho_1)) + d_I^2(d_I+2\rho_2+2z+\rho_1) \\ &\quad + \rho_1\rho_2(\rho_2+z)\} + (ps\beta(d_I+\rho_2+z) - cd_T\rho_1\rho_2)(d_I+z+\rho_2) + (ps\beta(d_I+\rho_2+z) - cd_T(d_I\rho_1+\rho_1\rho_2)(c+d_I)]. \end{aligned} \tag{16}$$

So, $k_5 > 0$ when $R_0 > 1$, and $(JUL)/cd_I(d_I + \rho_2 + z) > (QJ^2 + U^2)$.

We examine the characteristic polynomial of the Jacobian matrix evaluated at EE. All coefficients k_1, k_3, k_4, and k_5 are positive and satisfying the necessary condition for stability. Hence proved the EE E^* is locally asymptotically stable if $R_0 > 1$ and $(JUL)/cd_I(d_I + \rho_2 + z) > (QJ^2 + U^2)$. However, when $R_0 < 1$, the coefficient k_4 becomes negative, violating the Routh–Hurwitz conditions. So, E^* is unstable when $R_0 < 1$.

6. Numerical Simulations of the HBV Model

Numerical simulations were performed to validate the analytical results. Parameter values used or assessing the local stabilities of the DFE and EE are listed in Table 1. In our numerical simulations, we employed MATLAB's ode45 solver, local sensitivity analysis, and bifurcation analysis to explore the dynamics of the HBV infection model. The ode45 function is based on a variable-step Runge–Kutta method and is suitable for moderately stiff problems. To assess the impact of individual parameters on model output, we performed local sensitivity analysis by computing normalized sensitivity indices of the basic reproduction number R_0. Additionally, a bifurcation analysis was conducted to evaluate the qualitative behavior of the system near the critical threshold $R_0 = 1$. These combined approaches allowed us to assess both the stability properties and the parameter influence on viral dynamics.

Figure 2(a) presents the dynamics of three critical state variables in the HBV infection model when the basic reproduction number R_0 is approximately 0.912, which is below the epidemic threshold of 1. The simulation is carried out over a time span of 50 days, and the model tracks how the system evolves starting from an initial infection level. The first panel in Figure 2(a) shows the number of hepatocytes that carry a single copy of cccDNA, which corresponds to early or low-level HBV infection within cells. The plot indicates that I_1 remains near zero throughout the simulation. Even if a few cells become infected initially, the infection does not amplify due to insufficient viral transmission and replication, a result of $R_0 < 1$. The 2nd panel in Figure 2(a) represents hepatocytes containing multiple copies of cccDNA, signifying more advanced or productive infection stages. Like I_1, the population of I_2 fails to grow and decays to zero. This reflects the biological fact that without persistent infection, cells do not accumulate multiple cccDNA copies. The 3rd panel in Figure 2(a) shows the free virus concentration, denoted by V, shows a small initial value and then declines over time. Since both I_1 and I_2 remain negligible, there is minimal production of virus particles, and the natural clearance rate dominates, leading to elimination of the virus from the system. These results collectively demonstrate that the infection dies out across all compartments when $R_0 < 1$. Importantly, these figures provide numerical evidence for the local stability of the DFE: small initial perturbations decay over time, and the system returns to a healthy, uninfected state. This supports the theoretical result that maintaining $R_0 < 1$ is a critical condition for infection eradication. Figure 2(b) shows how the infection behaves over time when the basic reproduction number is greater than one ($R_0 \approx 1.6982e03$), meaning that the virus can spread and persist in the host. The three plots display the changes in single-copy infected cells (I_1), multiple-copy infected cells (I_2), and free virus (V). Each curve increases rapidly at first and then levels off, reaching a steady state, which indicates the system has settled at an EE. The vertical axis use a logarithmic scale to clearly show the wide range of values, especially during early growth. This behavior confirms the local stability of the EE, as all infected compartments remain positive over time.

The bifurcation diagram illustrates the behavior of three key compartments in the HBV infection model I_1 (single-copy cccDNA-infected cells), I_2 (multiple-copy cccDNA-infected cells), and V free virus (see Figure 3). The horizontal axis represents the variation in R_0, which is driven by changes in the infection rate β, while the vertical axis indicates the equilibrium levels of each compartment. Figure 3(a) indicates the level of infected population with single copy of cccDNA for values $R_0 < 1$, the infection cannot establish itself, and the system settles at the DFE with $I_1 = 0$. As soon as R_0 exceeds 1, the infection persists and a positive EE emerges, with I_1 increasing as R_0 increases. Figure 3(b) shows the multiple-copy cccDNA compartment I_2, which remains zero when $R_0 < 1$, indicating viral clearance, and increases with $R_0 > 1$, reflecting persistent infection and behaves similarly but with a different growth pattern due to its dependence on conversion from I_1. Figure 3(c) shows the dynamics of free virus (V), which also emerge only when $R_0 > 1$.

Figure 4 illustrates the variation of the basic reproduction number R_0 with respect to five key parameters: β, ρ_1, ρ_2, z, and d_I. Each subplot demonstrates how changes in a specific parameter affect R_0 while keeping other parameters constant. Figure 4(a) shows a linear increase in R_0 with increasing β, confirming a direct proportional relationship between transmission rate and R_0. In Figure 4(b), as ρ_1 increases, R_0 decreases, indicating that higher conversion rates of infected cells reduce overall transmission potential. Similarly, Figure 4(c) shows a decline in R_0 with increasing ρ_2, supporting its negative impact on the infection spread. In contrast, Figure 4(d) reveals that R_0 increases with higher values of z, suggesting that increased infection effectiveness (or increased reinfection) promotes disease transmission. Finally, Figure 4(e) demonstrates a clear negative relationship between d_I (infected cell death rate) and R_0, highlighting the suppressive effect of increased cell clearance on viral spread. The parameter ρ_1 (rate of transition from productively infected hepatocytes I_1 back to susceptible hepatocytes T) has a more pronounced impact on the infection dynamics compared to ρ_2 (rate of transition from refractory hepatocytes I_2 back to I_1).

7. Sensitivity Analysis of R_0 Using Normalized Sensitivity Indices

In practical scenarios, controlling disease prevalence is often limited by logistical or financial constraints [51, 52].

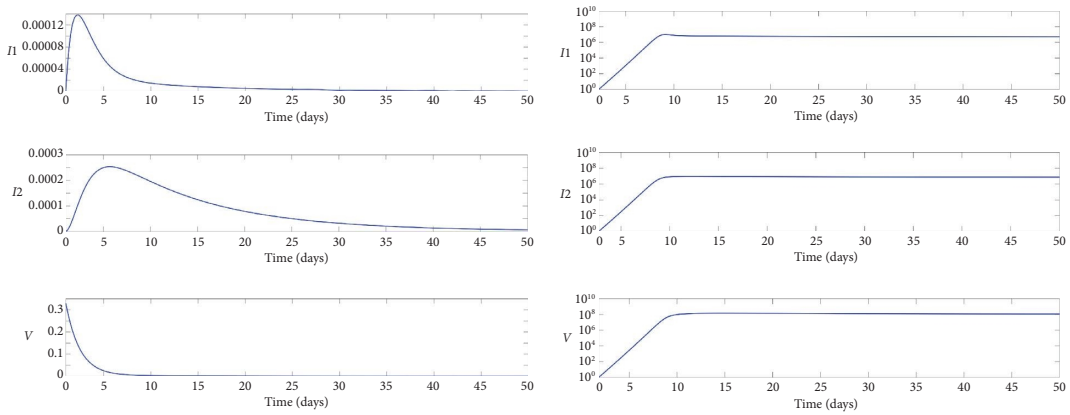

Figure 2: (a) Simulated time evolution of HBV infection states when the basic reproduction number is below the epidemic threshold ($R_0 \approx 0.912$). The first panel shows hepatocytes infected with a single copy of cccDNA (I_1), the second panel shows those with multiple copies of cccDNA (I_2), and the third displays the concentration of free virus particles (V). In all three cases, the state variables decay to zero, demonstrating that infection fails to establish and is cleared over time, consistent with the expected behavior under a forward bifurcation scenario with $R_0 < 1$. (b) Local stability of the EE for the same compartments, when the basic reproduction number is greater than one ($R_0 \approx 1.6982e03$), for the same compartments. The logarithmic scale on the vertical axis highlights the growth of viral and infected cell populations, and all trajectories converge to constant positive equilibrium values, confirming persistent infection dynamics under these conditions.

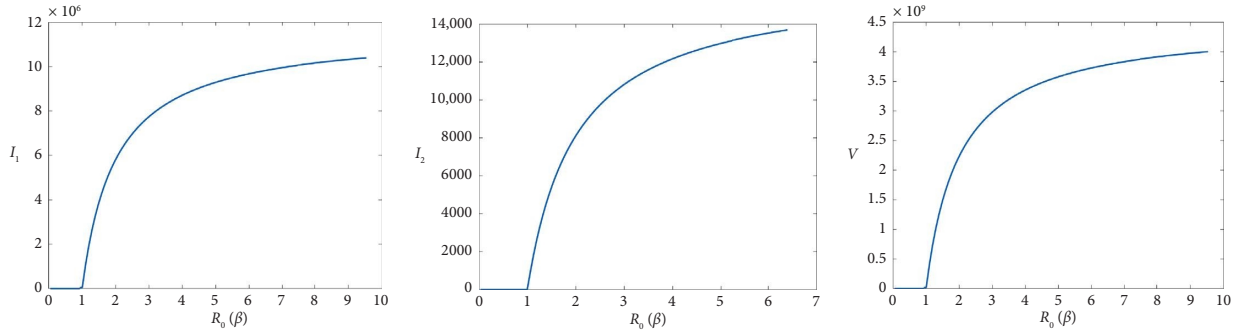

Figure 3: The bifurcation diagrams illustrate the behavior of three key compartments in the HBV infection model. (a) Single-copy cccDNA-infected cells (I_1), (b) multiple-copy cccDNA-infected cells (I_2), and (c) free virus (V). For $R_0 < 1$, infection cannot establish, and all compartments remain at zero. When $R_0 > 1$, infection persists with increasing levels of I_1, I_2, and V, reflecting the transition from disease-free to endemic equilibrium.

Therefore, identifying the most effective control measures to reduce disease spread is essential, with the ultimate goal of bringing R_0 below 1. Implementing such measures can alter certain model parameters, making it important to understand how each parameter influences R_0. To quantify these effects, we performed a sensitivity analysis of R_0 using normalized forward sensitivity indices. This method measures the relative change in R_0 caused by a relative change in each parameter, allowing direct comparison of their influence regardless of units or magnitude. Key parameters considered in this study include the transmission rate (β), the infected cell death rate (d_I), transition rate into the I_2 class (z), and ρ_1 and ρ_2 loss rate of infectious cells I_1 and I_2. Mathematically, sensitivity indices can be expressed as: $S_\beta = (\partial R_0/\partial\beta)\beta/R_0$, $S_{\rho_1} = (\partial R_0/\partial\rho_1)\rho_1/R_0$, $S_{\rho_2} = (\partial R_0/\partial\rho_2)\rho_2/R_0$, $S_z = (\partial R_0/\partial z)z/R_0$, and $S_{d_I} = (\partial R_0/\partial d_I)d_I/R_0$. These equations determine the sensitivity of R_0 to changes in the parameters. Figure 5 presents the sensitivity indices of the basic reproduction number R_0 with respect to key model parameters. These indices estimate the proportional change in R_0 resulting from a small proportional change in each parameter. The initial index $S_\beta = (\partial R_0/\partial\beta)(\beta/R_0) = 1$ remains constant, which means that every 1% change in parameter β has a direct and proportional effect on the transmission dynamics. As shown in Figures 5(a), 5(b), 5(d), the sensitivity indices for parameters ρ_1, ρ_2, and d_I are negative, implying that increases in these parameters lead to a decrease in R_0. Among them, d_I (the death rate of infected hepatocytes) exhibits the strongest negative impact on R_0, highlighting its importance in reducing transmission

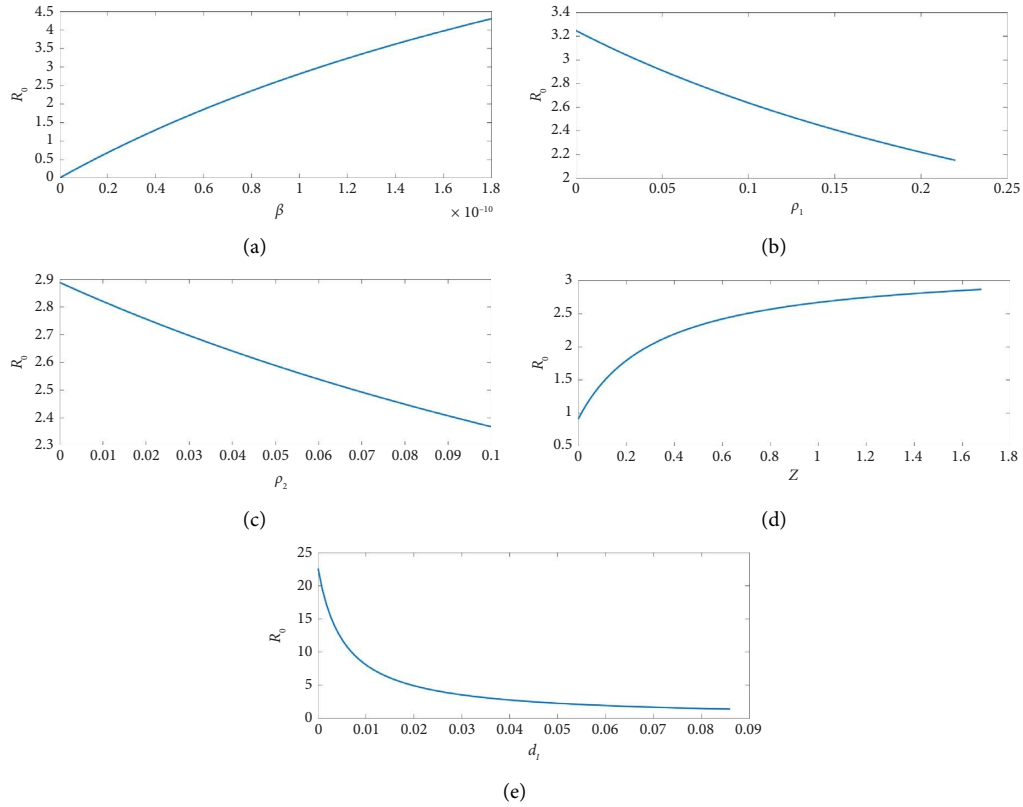

FIGURE 4: Illustration of the variation of the basic reproduction number R_0 with respect to changes in key model parameters. (a) Infection transmission rate from free virus to uninfected hepatocytes, β, (b) ρ_1 Rate of recycling from infected cells with one copy of cccDNA (I_1) to uninfected hepatocytes (T), (c) ρ_2 Rate of recycling from infected cells with multiple copies of cccDNA (I_2) back to singly infected cells (I_1), (d) z representing the transition from hepatocytes with a single copy of cccDNA (I_1) to multiple copies cccDNA (I_2), and (e) d_I death rate of infected hepatocytes. The x-axis represents individual parameter values (β, ρ_1, ρ_2, z, and d_I), and the y-axis shows the corresponding R_0. This provides visual insight into which parameters most influence the dynamics of R_0. Positive and negative slopes indicate parameters that increase or decrease R_0, respectively.

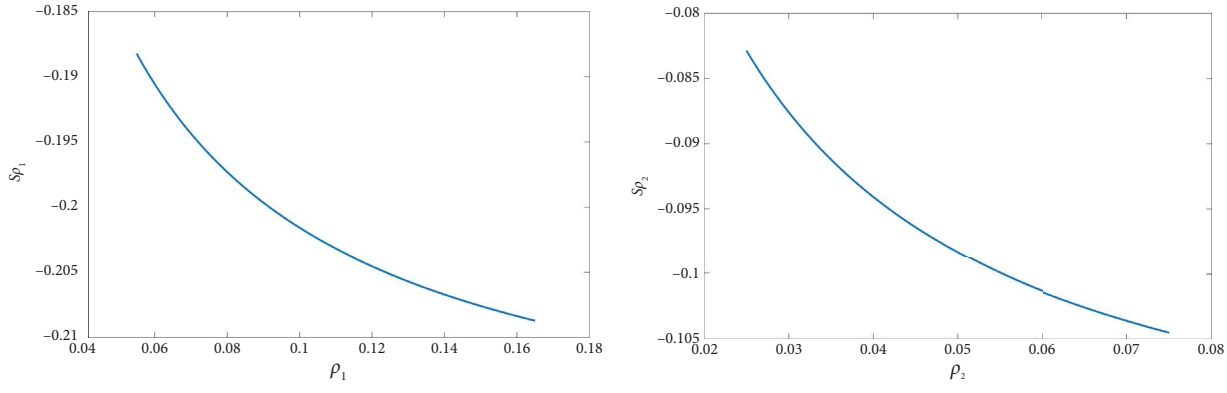

FIGURE 5: Continued.

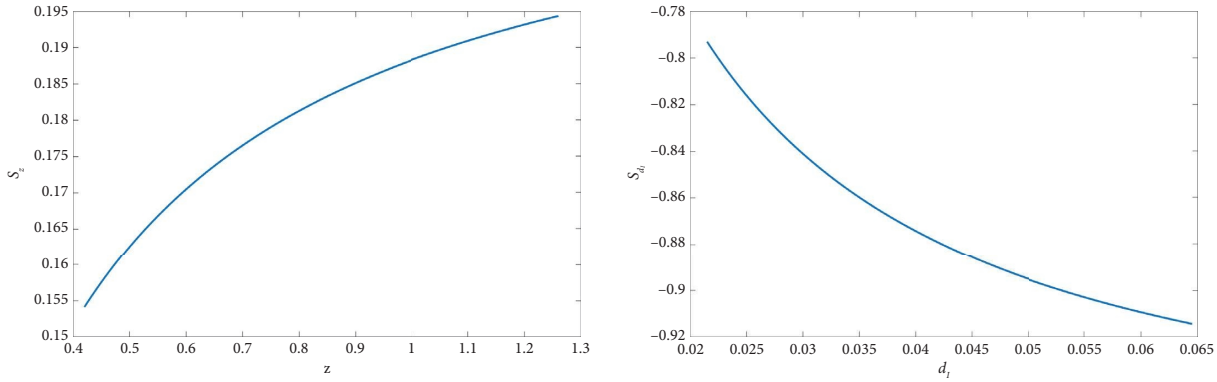

(c) (d)

FIGURE 5: Sensitivity indices with respect to key parameters. (a) Sensitivity index S_{ρ_1} versus ρ_1, (b) sensitivity index S_{ρ_2} versus ρ_2, (c) sensitivity index S_z versus z, (d) sensitivity index S_{d_I} versus d_I. The y-axis in each plot represents the normalized sensitivity index, indicating the relative impact of each parameter on the model output.

potential. Figure 5(c) shows a positive sensitivity index for parameter z, suggesting that increasing the rate z enhances R_0, thus potentially accelerating disease transmission. The ranges for the analyzed parameters are as follows: ρ_1 (0.055–0.165), ρ_2 (0.025–0.075), d_I (0.0215–0.0645), and z (0.42–1.26). These findings identify which parameters most influence transmission dynamics and provide insight into which biological processes have the strongest impact.

8. Discussion and Conclusion

Despite extensive efforts to model HBV infection mathematically, significant gaps in representing its intracellular complexity persist. For instance, the model by Ciupe et al. introduced the terms ρ_1 and ρ_2, but these were studied only in the presence of complex immune dynamics [48]. As a result, the independent role of cccDNA recycling in HBV persistence was never fully isolated or mathematically characterized. Similarly, other models (e.g., Kim et al. and subsequent therapy-based models [49, 53]) have primarily focused on antiviral drug effects [54] or explicit immune responses [55], while treating infected hepatocytes as a single compartment without distinguishing between intracellular cccDNA burdens. This simplification overlooks experimental evidence, showing that hepatocytes harboring multiple cccDNA copies exhibit greater persistence and reactivation potential compared to those with a single copy (single-cell analyses report average cccDNA copy numbers between 6 and 60 per hepatocyte [22], clinical data demonstrate that cccDNA persists long-term despite antiviral therapy [26], reviews emphasize the role of persistent intracellular cccDNA reservoirs in reactivation risk [20]). To the best of our knowledge, no study has provided a mathematical framework that isolates the impact of recycling dynamics on HBV infection while excluding immune complexity. Addressing this gap is crucial because it enables a clearer understanding of how intercellular transitions between single- and multiple-copy states influence stability, viral persistence, and potential therapeutic strategies.

The HBV recycling lifecycle is highly complex, involving multiple intracellular and extracellular processes that influence persistence and disease. Progression. This complexity makes it challenging to pinpoint the parameters most critical for infection propagation. To address this issue, our study proposed and analyzed a mathematical model that explicitly incorporates intracellular heterogeneity by dividing infected hepatocytes into compartments with either a single copy (I_1) or multiple copies (I_2) of cccDNA, in addition to uninfected hepatocytes (T) and free virus (V). The inclusion of recycling parameters (ρ_1 and ρ_2) allowed us to capture transitions between these infected states, representing biologically relevant processes such as partial immune-mediated clearance and cccDNA amplifications.

Our stability analysis demonstrated that when $R_0 < 1$, the DFE is locally asymptotically stable, while $R_0 > 1$ leads to a stable EE. Numerical simulations supported these analytical results, with computed R_0 values matching predicted stability outcomes. Sensitivity analysis revealed that fluctuations in β, ρ_1, ρ_2, z, and d_I substantially influence R_0. We observed that ρ_1, ρ_2, and d_I are particularly effective for reducing HBV infections, while the other parameters tend to increase the rate of infection.

The parameter ρ_1 has a more pronounced impact on the infection dynamics compared to ρ_2. Increasing ρ_1 accelerates the clearance of I_1 cells, thereby reducing the overall production of virus and lowering the basic reproduction number R_0 more effectively. In contrast, changes in ρ_2 primarily influence the recycling of I_2 back into the I_1 compartment, which has a more indirect and generally weaker effect on R_0 and the long-term viral load. As a result, variations in ρ_1 lead to more substantial shifts in steady-state virus levels and infection persistence than equivalent changes in ρ_2. Although ρ_1 is not a directly targetable biochemical reaction, it may capture the rate of noncytolytic clearance or reversion of hepatocytes harboring a single copy of cccDNA (I_1). While introduced as a mathematical parameter, ρ_1 is biologically interpretable and can indeed be influenced by therapeutic strategies. Specifically, ρ_1 reflects

processes such as (i) immune-mediated degradation of cccDNA (e.g., interferon-α stimulation), (ii) transcriptional silencing of cccDNA, and (iii) novel therapeutic interventions that destabilize or reduce cccDNA activity without killing hepatocytes. Recent studies have demonstrated that cccDNA can be selectively silenced or degraded in hepatocytes through interferon stimulation, RNA-targeting approaches, or capsid assembly inhibitors [56–58]. These findings strengthen the practical relevance of our sensitivity analysis, which shows that increasing ρ_1 has a particularly strong impact on HBV suppression, highlighting it as a promising therapeutic target.

Despite the comprehensive nature of our model, one notable limitation is its simplification and omission of intracellular mechanisms, which can significantly affect HBV dynamics. We did not consider the intricate processes occurring inside cells, such as viral replication, transcription, and translation. These intracellular mechanisms play a crucial role in HBV infection dynamics and immune response; however, we were not included in our model because of their complexity. Another limitation is that parameter values used in the model were sourced from the literature because of the absence of the data for parameter estimation. Our model may not fully capture the intricate interplay between viral replication, host immune response, and therapeutic interventions. Another limitation is that we only estimated the sensitivity index value, which represents local sensitivity rather than global sensitivity, because it is calculated solely from the estimated parameter values.

Future extensions of the model will include more detailed intracellular processes such as cccDNA transcriptional regulation and epigenetic silencing, as well as immune components including cytotoxic T lymphocyte responses and natural killer cell activity. We also aim to incorporate PK and pharmacodynamic (PD) dynamics to simulate the clinical impact of antiviral agents. Furthermore, an important direction for future work will be to fit the model to experimental or patient-specific data to estimate parameters more accurately, validate model predictions, and enable personalized treatment simulations. These enhancements will improve the biological realism and translational relevance of the model for therapeutic design and HBV management.

In conclusion, this study presents a novel mathematical model that distinguishes between hepatocytes harboring a single copy (I_1) and multiple copies (I_1) of cccDNA, providing a biologically realistic representation of intracellular HBV infection dynamics. By incorporating recycling parameters (ρ_1 and ρ_2), the model captures key processes such as noncytolytic immune clearance, cccDNA reversion, and intracellular regulation features often neglected in traditional HBV models. This extended structure enables a more accurate derivation of the basic reproduction number (R_0) and improves understanding of how intracellular heterogeneity influences infection persistence. Sensitivity and bifurcation analyses further demonstrate that early interventions, particularly those enhancing ρ_1, may be more effective in controlling HBV than treatments focused on later infection stages.

Data Availability Statement

This study did not generate or analyze any new data.

Conflicts of Interest

The authors declare no conflicts of interest.

Author Contributions

Malik Muhammad Ibrahim conceptualized, designed, implemented, drafted, critically revised, and approved the final version of the manuscript. Jong Hyuk Byun, Malik Muhammad Naeem Mannan, and Il Hyo Jung contributed to the implementation, drafting, critical revision, and approval of the final version of the manuscript. Kwang Su Kim contributed to the conceptualization, critical revision, and approval of the final version of the manuscript. Malik Muhammad Ibrahim and Jong Hyuk Byun contributed equally to this study.

Funding

This work was supported by the National Research Foundation of Korea (NRF) grant funded by the Korea government (MSIT) (2022R1C1C2003637to Kwang Su Kim, No. RS-2023-00210403 to Jong Hyuk Byun, and No. RS-2024-00342113 to Il Hyo Jung). This work was supported by the Global Joint Research Program funded by the Pukyong National University (202411510001 to Kwang Su Kim) and Learning & Academic research institution for Master's·PhD students, and Postdocs (LAMP) Program of the National Research Foundation of Korea (NRF) grant funded by the Ministry of Education (No. RS-2023-00301938 to Jong Hyuk Byun).

Acknowledgments

This work was supported by the National Research Foundation of Korea (NRF) grant funded by the Korea government (MSIT) (2022R1C1C2003637 to K.S.K., No. RS-2023-00210403 to JHB, No. RS-2024-00342113 to ILJ). This work was supported by the Global Joint Research Program funded by the Pukyong National University (202411510001 to K.S.K) and Learning & Academic research institution for Master's·PhD students, and Postdocs (LAMP) Program of the National Research Foundation of Korea (NRF) grant funded by the Ministry of Education (No. RS-2023-00301938 to JHB).

References

[1] C. W. Shepard, E. P. Simard, L. Finelli, A. E. Fiore, and B. P. Bell, "Hepatitis B Virus Infection: Epidemiology and Vaccination," *Epidemiologic Reviews* 28, no. 1 (2006): 112–125, https://doi.org/10.1093/epirev/mxj009.

[2] B. Rehermann and M. Nascimbeni, "Immunology of Hepatitis B Virus and Hepatitis C Virus Infection," *Nature Reviews Immunology* 5, no. 3 (2005): 215–229, https://doi.org/10.1038/nri1573.

[3] Y. Ishida, T. L. Chung, M. Imamura, et al., "Acute Hepatitis B Virus Infection in Humanized Chimeric Mice Has Multiphasic Viral Kinetics," *Hepatology* 68, no. 2 (2018): 473–484, https://doi.org/10.1002/hep.29891.

[4] C. W. Shepard, L. Finelli, and M. J. Alter, "Global Epidemiology of Hepatitis C Virus Infection," *The Lancet Infectious Diseases* 5, no. 9 (2005): 558–567, https://doi.org/10.1016/S1473-3099(05)70216-4.

[5] X. Chen, C. Fu, J. Liu, L. Shan, and C. Liu, "Recent Epidemiological and Clinical Features of Acute Hepatitis B in a Single Center of China," *International Journal of Clinical and Experimental Medicine* 8, no. 9 (2015): 16652.

[6] H. Yan, G. Zhong, G. Xu, et al., "Sodium Taurocholate Cotransporting Polypeptide is a Functional Receptor for Human Hepatitis B and D Virus," *Elife* 1 (2012): e00049, https://doi.org/10.7554/eLife.00049.

[7] K. Watashi, S. Urban, W. Li, and T. Wakita, "NTCP and Beyond: Opening the Door to Unveil Hepatitis B Virus Entry," *International Journal of Molecular Sciences* 15, no. 2 (2014): 2892–2905, https://doi.org/10.3390/ijms15022892.

[8] R. J. Lamontagne, S. Bagga, and M. J. Bouchard, "Hepatitis B Virus Molecular Biology and Pathogenesis," *Hepatoma research* 2, no. 7 (2016): 163, https://doi.org/10.20517/2394-5079.2016.05.

[9] C. Seeger and W. S. Mason, "Molecular Biology of Hepatitis B Virus Infection," *Virology* 479-480 (2015): 672–686, https://doi.org/10.1016/j.virol.2015.02.031.

[10] M.-L. Blondot, V. Bruss, and M. Kann, "Intracellular Transport and Egress of Hepatitis B Virus," *Journal of Hepatology* 64, no. 1 (2016): S49–S59, https://doi.org/10.1016/j.jhep.2016.02.008.

[11] M. Nassal, "Hepatitis B Viruses: Reverse Transcription a Different Way," *Virus Research* 134, no. 1-2 (2008): 235–249, https://doi.org/10.1016/j.virusres.2007.12.024.

[12] N. A. Terrault, N. H. Bzowej, K. M. Chang, J. P. Hwang, M. M. Jonas, and M. H. Murad, "A ASLD Guidelines for Treatment of Chronic Hepatitis B," *Hepatology* 63, no. 1 (2016): 261–283, https://doi.org/10.1002/hep.28156.

[13] N. Ruiz-Opazo, P. R. Chakraborty, and D. A. Shafritz, "Evidence for Supercoiled Hepatitis B Virus DNA in Chimpanzee Liver and Serum Dane Particles: Possible Implications in Persistent HBV Infection," *Cell* 29, no. 1 (1982): 129–138, https://doi.org/10.1016/0092-8674(82)90097-6.

[14] J. Summers and W. S. Mason, "Replication of the Genome of a Hepatitis B-like Virus by Reverse Transcription of an RNA Intermediate," *Cell* 29, no. 2 (1982): 403–415, https://doi.org/10.1016/0092-8674(82)90157-X.

[15] W. S. Mason, C. Aldrich, J. Summers, and J. M. Taylor, "Asymmetric Replication of Duck Hepatitis B Virus DNA in Liver Cells: Free minus-strand DNA," *Proceedings of the National Academy of Sciences* 79, no. 13 (1982): 3997–4001, https://doi.org/10.1073/pnas.79.13.3997.

[16] J. S. Tuttleman, C. Pourcel, and J. Summers, "Formation of the Pool of Covalently Closed Circular Viral DNA in hepadnavirus-infected Cells," *Cell* 47, no. 3 (1986): 451–460, https://doi.org/10.1016/0092-8674(86)90602-1.

[17] A. Zhu, X. Liao, S. Li, et al., "HBV Cccdna and Its Potential as a Therapeutic Target," *Journal of Clinical and Translational Hepatology* 7, no. X (2019): 1–5, https://doi.org/10.14218/JCTH.2018.00054.

[18] D. H. Kim, H. S. Kang, and K.-H. Kim, "Roles of Hepatocyte Nuclear Factors in Hepatitis B Virus Infection," *World Journal of Gastroenterology* 22, no. 31 (2016): 7017, https://doi.org/10.3748/wjg.v22.i31.7017.

[19] Q. Huang, B. Zhou, D. Cai, et al., "Rapid Turnover of Hepatitis B Virus Covalently Closed Circular DNA Indicated by Monitoring Emergence and Reversion of Signature-Mutation in Treated Chronic Hepatitis B Patients," *Hepatology* 73, no. 1 (2021): 41–52, https://doi.org/10.1002/hep.31240.

[20] F. Zoulim, "New Insight on Hepatitis B Virus Persistence from the Study of Intrahepatic Viral Cccdna," *Journal of Hepatology* 42, no. 3 (2005): 302–308, https://doi.org/10.1016/j.jhep.2004.12.015.

[21] J.-T. Guo and H. Guo, "Metabolism and Function of Hepatitis B Virus Cccdna: Implications for the Development of cccDNA-targeting Antiviral Therapeutics," *Antiviral Research* 122 (2015): 91–100, https://doi.org/10.1016/j.antiviral.2015.08.005.

[22] Y.-Y. Zhang, B.-H. Zhang, D. Theele, S. Litwin, E. Toll, and J. Summers, "Single-Cell Analysis of Covalently Closed Circular DNA Copy Numbers in a hepadnavirus-infected Liver," *Proceedings of the National Academy of Sciences* 100, no. 21 (2003): 12372–12377, https://doi.org/10.1073/pnas.2033898100.

[23] S. Bowden, S. Locarnini, T. T. Chang, et al., "Covalently closed-circular Hepatitis B Virus DNA Reduction with Entecavir or Lamivudine," *World Journal of Gastroenterology* 21, no. 15 (2015): 4644–4651, https://doi.org/10.3748/wjg.v21.i15.4644.

[24] J. J. Y. Sung, M. L. Wong, S. Bowden, et al., "Intrahepatic Hepatitis B Virus Covalently Closed Circular DNA Can Be a Predictor of Sustained Response to Therapy," *Gastroenterology* 128, no. 7 (2005): 1890–1897, https://doi.org/10.1053/j.gastro.2005.03.009.

[25] K. Wursthorn, M. Lutgehetmann, M. Dandri, et al., "Peginterferon alpha-2b plus Adefovir Induce Strong Cccdna Decline and Hbsag Reduction in Patients with Chronic Hepatitis B," *Hepatology* 44, no. 3 (2006): 675–684, https://doi.org/10.1002/hep.21282.

[26] B. Werle–Lapostolle, S. Bowden, S. Locarnini, K. Wursthorn, J. Petersen, et al., "Persistence of Cccdna During the Natural History of Chronic Hepatitis B and Decline During Adefovir Dipivoxil Therapy," *Gastroenterology* 126, no. 7 (2004): 1750–1758, https://doi.org/10.1053/j.gastro.2004.03.018.

[27] M. Gümüş and K. Türk, "Dynamical Behavior of a Hepatitis B Epidemic Model and Its NSFD Scheme," *Journal of Applied Mathematics and Computing* 70, no. 4 (2024): 3767–3788, https://doi.org/10.1007/s12190-024-02103-6.

[28] M. Gümüş and K. Türk, "Global Analysis of a Monkeypox Virus Model Considering Government Interventions," *Physica Scripta* 100, no. 4 (2025): 045216, https://doi.org/10.1088/1402-4896/ada318.

[29] M. A. Nowak, S. Bonhoeffer, A. M. Hill, R. Boehme, H. C. Thomas, and H. McDade, "Viral Dynamics in Hepatitis B Virus Infection," *Proceedings of the National Academy of Sciences* 93, no. 9 (1996): 4398–4402, https://doi.org/10.1073/pnas.93.9.4398.

[30] A. Din, "Bifurcation Analysis of a Delayed Stochastic HBV Epidemic Model: Cell-To-Cell Transmission," *Chaos, Solitons & Fractals* 181 (2024): 114714, https://doi.org/10.1016/j.chaos.2024.114714.

[31] A. Din and Y. Li, "Optimizing HIV/AIDS Dynamics: Stochastic Control Strategies with Education and Treatment," *The European Physical Journal Plus* 139, no. 9 (2024): 812, https://doi.org/10.1140/epjp/s13360-024-05605-1.

[32] W. Ali Khan, R. Zarin, A. Zeb, Y. Khan, and A. Khan, "Navigating Food Allergy Dynamics via a Novel Fractional Mathematical Model for antacid-induced Allergies," *Journal*

of Mathematical Techniques in Modeling 1, no. 1 (2024): 25–51, https://doi.org/10.56868/jmtm.v1i1.3.

[33] S. Shah, H. Tahir, A. Khan, W. A. Khan, and A. Arshad, "Stochastic Model on the Transmission of Worms in Wireless Sensor Network," *Journal of Mathematical Techniques in Modeling* 1, no. 1 (2024): https://doi.org/10.56868/jmtm.v1i1.31.

[34] Q. tul Ain, "Nonlinear Stochastic Cholera Epidemic Model Under the Influence of Noise," *Journal of Mathematical Techniques in Modeling* 1, no. 1 (2024): https://doi.org/10.56868/jmtm.v1i1.30.

[35] S. Ullah, "Investigating a Coupled System of Mittag-Leffler Type Fractional Differential Equations with Coupled Integral Boundary Conditions," *J. Math. Tech. Model* 1, no. 2 (2024): 16–28.

[36] J. P. Chauhan, S. R. Khirsariya, B. M. Yeolekar, and M. A. Yeolekar, "Fractional Mathematical Model of Listeria Infection Caused by Pre-cooked Package Food," *Results in Control and Optimization* 14 (2024): 100371, https://doi.org/10.1016/j.rico.2024.100371.

[37] P. A. Naik, B. M. Yeolekar, S. Qureshi, et al., "Global Analysis of a Fractional-Order Hepatitis B Virus Model Under Immune Response in the Presence of Cytokines," *Advanced Theory and Simulations* 7, no. 12 (2024): 2400726, https://doi.org/10.1002/adts.202400726.

[38] P. A. Naik, B. M. Yeolekar, S. Qureshi, M. Yeolekar, and A. Madzvamuse, "Modeling and Analysis of the fractional-order Epidemic Model to Investigate Mutual Influence in HIV/HCV co-infection," *Nonlinear Dynamics* 112, no. 13 (2024): 11679–11710, https://doi.org/10.1007/s11071-024-09653-1.

[39] P. A. Naik, B. M. Yeolekar, S. Qureshi, M. Yavuz, Z. Huang, and M. Yeolekar, "Fractional Insights in Tumor Modeling: an Interactive Study Between Tumor Carcinogenesis and Macrophage Activation," *Advanced Theory and Simulations* 8, no. 7 (2025): 2401477, https://doi.org/10.1002/adts.202401477.

[40] A. Murase, T. Sasaki, and T. Kajiwara, "Stability Analysis of pathogen-immune Interaction Dynamics," *Journal of Mathematical Biology* 51, no. 3 (2005): 247–267, https://doi.org/10.1007/s00285-005-0321-y.

[41] V. A. Sypsa, K. Mimidis, N. C. Tassopoulos, et al., "A Viral Kinetic Study Using Pegylated Interferon alfa-2b and/or Lamivudine in Patients with Chronic Hepatitis B/HBeAg Negative," *Hepatology* 42, no. 1 (2005): 77–85, https://doi.org/10.1002/hep.20738.

[42] S. Eikenberry, S. Hews, J. D. Nagy, and Y. Kuang, "The Dynamics of a Delay Model of Hepatitis B Virus Infection with Logistic Hepatocyte Growth," *Mathematical Biosciences and Engineering: MBE* 6, no. 2 (2009): 283–299, https://doi.org/10.3934/mbe.2009.6.283.

[43] K. Wang, W. Wang, and S. Song, "Dynamics of an HBV Model with Diffusion and Delay," *Journal of Theoretical Biology* 253, no. 1 (2008): 36–44, https://doi.org/10.1016/j.jtbi.2007.11.007.

[44] B.-Z. Guo and L.-M. Cai, "A Note for the Global Stability of a Delay Differential Equation of Hepatitis B Virus Infection," *Mathematical Biosciences and Engineering: MBE* 8, no. 3 (2011): 689–694, https://doi.org/10.3934/mbe.2011.8.689.

[45] S. A. Gourley, Y. Kuang, and J. D. Nagy, "Dynamics of a Delay Differential Equation Model of Hepatitis B Virus Infection," *Journal of Biological Dynamics* 2, no. 2 (2008): 140–153, https://doi.org/10.1080/17513750701769873.

[46] G. Huang, Y. Takeuchi, and W. Ma, "Lyapunov Functionals for Delay Differential Equations Model of Viral Infections," *SIAM Journal on Applied Mathematics* 70, no. 7 (2010): 2693–2708, https://doi.org/10.1137/090780821.

[47] Q. Li, F. Lu, G. Deng, and K. Wang, "Modeling the Effects of Covalently Closed Circular DNA and Dendritic Cells in Chronic HBV Infection," *Journal of Theoretical Biology* 357 (2014): 1–9, https://doi.org/10.1016/j.jtbi.2014.04.037.

[48] S. M. Ciupe, R. M. Ribeiro, P. W. Nelson, and A. S. Perelson, "Modeling the Mechanisms of Acute Hepatitis B Virus Infection," *Journal of Theoretical Biology* 247, no. 1 (2007): 23–35, https://doi.org/10.1016/j.jtbi.2007.02.017.

[49] H. Y. Kim, H.-D. Kwon, T. S. Jang, J. Lim, and H.-S. Lee, "Mathematical Modeling of Triphasic Viral Dynamics in Patients with HBeAg-positive Chronic Hepatitis B Showing Response to 24-week Clevudine Therapy," *PLoS One* 7, no. 11 (2012): e50377, https://doi.org/10.1371/journal.pone.0050377.

[50] M. M. Ibrahim, M. A. Kamran, M. M. Naeem Mannan, S. Kim, and I. H. Jung, "Impact of Awareness to Control Malaria Disease: a Mathematical Modeling Approach," *Complexity* 2020, no. 1 (2020): 1–13, https://doi.org/10.1155/2020/8657410.

[51] C. Hutchison, M. Khan, J. Yoong, X. Lin, and R. Coker, "Financial Barriers and Coping Strategies: a Qualitative Study of Accessing multidrug-resistant Tuberculosis and Tuberculosis Care in Yunnan, China," *BMC Public Health* 17, no. 1 (2017): 221, https://doi.org/10.1186/s12889-017-4089-y.

[52] Y. Tao, K. Shea, and M. Ferrari, "Logistical Constraints Lead to an Intermediate Optimum in Outbreak Response Vaccination," *PLoS Computational Biology* 14, no. 5 (2018): e1006161, https://doi.org/10.1371/journal.pcbi.1006161.

[53] M. Tsiang, J. F. Rooney, J. J. Toole, and C. S. Gibbs, "Biphasic Clearance Kinetics of Hepatitis B Virus From Patients During Adefovir Dipivoxil Therapy," *Hepatology* 29, no. 6 (1999): 1863–1869, https://doi.org/10.1002/hep.510290626.

[54] Y. Ding and W. J. Wang, "Control Strategy Design for the Anti-Hbv Mathematical Model," *IET Systems Biology* 13, no. 4 (2019): 186–193, https://doi.org/10.1049/iet-syb.2019.0023.

[55] F. Fatehi Chenar, Y. Kyrychko, and K. Blyuss, "Mathematical Model of Immune Response to Hepatitis B," *Journal of Theoretical Biology* 447 (2018): 98–110, https://doi.org/10.1016/j.jtbi.2018.03.025.

[56] J. Lucifora, Y. Xia, F. Reisinger, et al., "Specific and Nonhepatotoxic Degradation of Nuclear Hepatitis B Virus Cccdna," *Science* 343, no. 6176 (2014): 1221–1228, https://doi.org/10.1126/science.1243462.

[57] F. Zoulim and S. Locarnini, "Hepatitis B Virus Resistance to Nucleos (T) Ide Analogues," *Gastroenterology* 137, no. 5 (2009): 1593–1608, https://doi.org/10.1053/j.gastro.2009.08.063.

[58] P. A. Revill, F. V. Chisari, J. M. Block, et al., "A Global Scientific Strategy to Cure Hepatitis B," *The lancet Gastroenterology & hepatology* 4, no. 7 (2019): 545–558, https://doi.org/10.1016/S2468-1253(19)30119-0.